PAPER REF: 3893

INFLUENCE OF THE POISSON'S RATIO ON FRACTURE PARAMETERS IN FUNCTIONALLY GRADED MATERIALS

Emilio Martínez-Pañeda[1(*)], Rafael Gallego[2]

[1]Department of Civil and Mechanical Engineering, University of Oviedo, Gijón, Spain.
[2]Department of Structural Mechanics and Hydraulic Engineering, University of Granada, Granada, Spain.
[(*)]*Email:* martinezemilio@uniovi.es

ABSTRACT

This work investigates the Poisson's ratio effect on the fracture process of functionally graded materials (FGMs). In order to develop a general scheme, an experimental case involving the three characteristic geometries of mixed-mode fracture in FGMs is simulated by means of the finite element method. Computational results of fracture parameters are compared to available experimental data and good agreement is obtained. Afterwards, stress intensity factors (SIFs) and *T*-stress are computed for different values of the Poisson's ratio, which either remains constant or continuously varies through the specimen. Results show that Poisson's ratio influence is highly dependent on the configuration evaluated.

Keywords: Functionally graded material (FGM), Poisson's ratio, fracture mechanics, finite element method (FEM).

INTRODUCTION

Functionally Graded Materials (FGMs) are those whose composition and hence their properties vary gradually as a function of the position. With growing applications of FGMs, research on fracture behavior of these non-homogeneous solids has generated considerable interest (Tilbrook, 2003). The primary conclusion of these investigations is that the classical inverse square root singular nature of the stress field is preserved in FGMs, but fracture parameters are influenced by the non-homogeneity of the material. Although the effect in the fracture behavior of the Young's Modulus variation has been thoroughly investigated, the influence on the near crack-tip fields of a spatial variation of the Poisson's ratio has not received the attention of the scientific community and its effect on the results is usually neglected based on Delale and Erdogan's conclusions (Delale, 1983). Nevertheless, their work considered only the case where tension load is applied in the direction perpendicular to material gradation and, as the more compliant part of the material may show more contraction than the stiffer part when tension load is applied in the direction *parallel* to material gradation, Poisson's ratio effect could be dependent on the analyzed geometry.

Paulino and Kim (Paulino, 2004) have already warned of the inaccuracies arising from the assumption of a constant Poisson's ratio in fracture analysis of FGMs, although they have only considered the most favorable configuration for the Poisson's ratio influence and an exponential or hyperbolic Young's modulus variation, i.e. a steeper variation than in a real case, resulting in a greater influence of the Poisson's ratio in the fracture parameters. Therefore, a comprehensive analysis of the Poisson's ratio effect as a function of the geometry with a more prevalent shape of the elastic gradient is needed in order to rate its relevance on practical engineering failure problems.

In the present work the experimental test of Abanto-Bueno and Lambros (Abanto-Bueno, 2006) is simulated through the finite element method, and once validated, the numerical model is developed in order to analyze the influence of a spatial variation of the Poisson's ratio, either by comparing the results obtained for different constant values or by considering a continuously variation of its value through the specimen evaluated.

MODEL FORMULATION

The experimental results reported in this work are taken from those obtained by Abanto-Bueno and Lambros (Abanto-Bueno, 2006). They manufactured polymeric model FGMs based on selective ultraviolet (UV) irradiation of polyethylene cocarbon monoxide (ECO). ECO is a very ductile semicrystalline copolymer that undergoes accelerated mechanical degradation when exposed to UV light, so that by gradually irradiating a sheet of the material from one end to the other, a sample with continuous in-plane property gradation from stiff and brittle to more compliant and more ductile can be obtained. A very thin sheet is irradiated gradually for times varying from 5 h to 300 h and subsequently cut in two halves, parallel to the irradiation direction. One of these samples is then divided in small strips that are subjected to uniaxial tension tests in order to measure the material property variation as a function of the position. The remaining sample is used to generate SENT fracture specimens so that the material property variation is measured independently of the fracture experiments, but originating from the same manufacturing process.

Abanto-Bueno and Lambros' experimental work (Abanto-Bueno, 2006) is well suited to develop a complete methodology as it involves the three characteristic geometries of mixed-mode fracture in FGMs. Mixed-mode fracture is inherent to FGMs since for a crack inclined to the property gradation direction, the stress state near the crack tip is mixed-mode irrespective of the far field loading. Thereby, near-tip mixity can be attained either by asymmetric external loading, or by placing the notch at an angle to the direction of mechanical property variation, or by a combination of both. The effect of each of these cases is investigated using three specimens labeled here FGM I, II and III. The geometry, dimensions and measured variation of elastic properties of the three specimens are shown in Table 1 and Fig. 1.

Table 1 Dimensions of the FGM specimens

	H [mm]	**W [mm]**	**h [mm]**	**a [mm]**	**φ [rad]**
FGMI	75	70	37.5	30	$\pi/2$
FGMII	90	70	32	26	$\pi/3$
FGMIII	90	70	32	25	$\pi/3$

Numerical simulations were conducted using the commercially available ABAQUS finite element software. Mimicking the experimental procedure, loading is applied as a fixed vertical displacement along the upper edge of the specimen, the displacement boundary condition is prescribed such that the vertical displacement is set to zero in the lower edge and in order to remove rigid body motion, the horizontal displacement is set to zero at the lower right hand corner. Following Abanto-Bueno and Lambros' criteria (Abanto-Bueno, 2006), plane stress conditions and a linear elastic behavior are assumed.

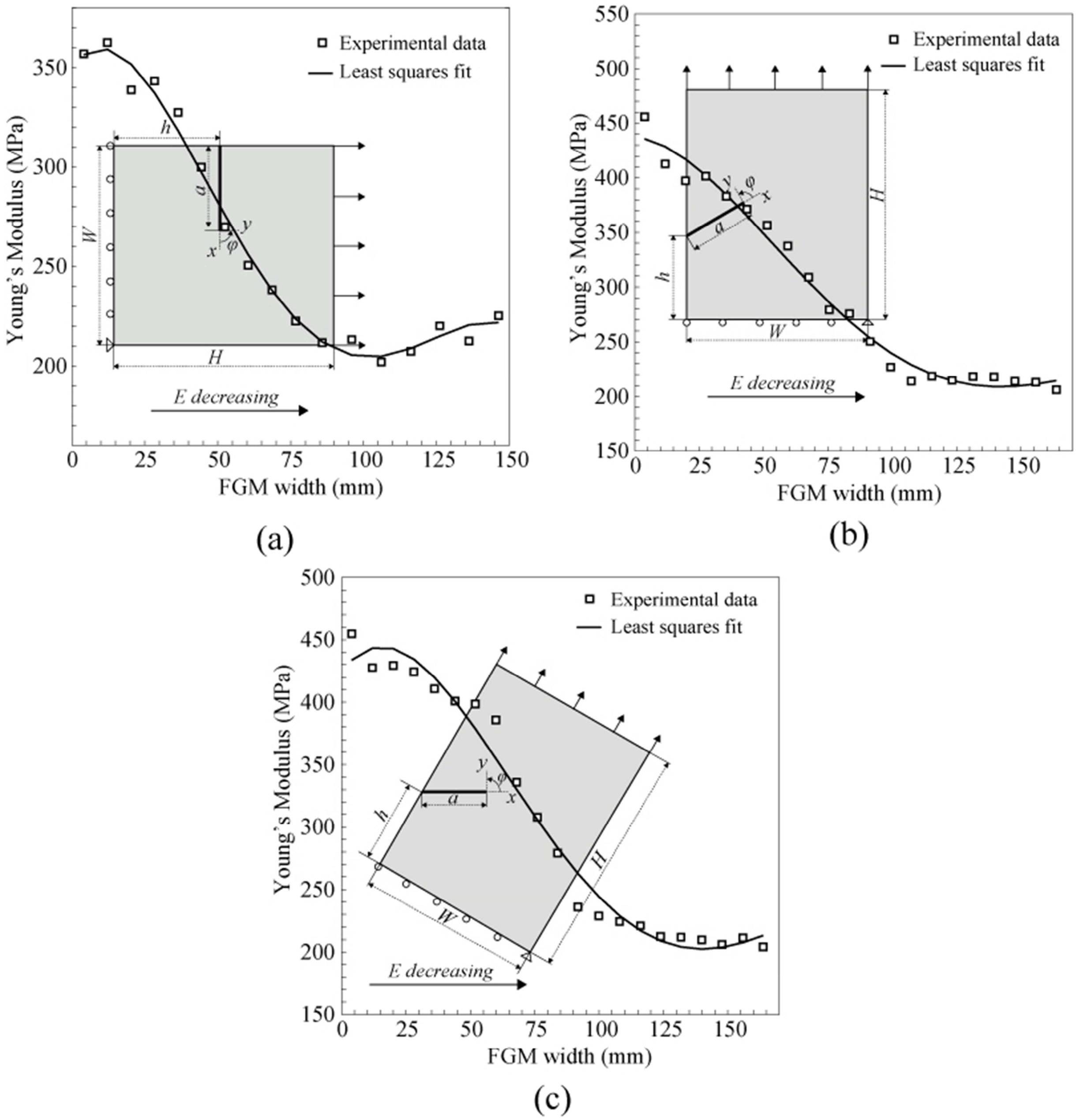

Fig.1 Geometry, dimensions and measured variation of the elastic properties as a function of the width of **(a)** FGMI, **(b)** FGMII and **(c)** FGMIII

The assignment of material properties must reflect the property distribution of the specimen being simulated. In the present work spatially-varying properties are assigned at integration points employing temperature-dependent data properties (Rousseau, 2000). Temperature dependent modulus is assumed and the material is provided with an initial temperature distribution to match the desired elastic modulus variation.

A constant value of ν=0.45 is considered for the Poisson's ratio, as it was also assumed in the data analysis of Abanto-Bueno and Lambros (Abanto-Bueno, 2006). This value was taken from the literature since the effect of the UV irradiation on Poisson's ratio is unknown and, because of the nature of the ECO specimens, they were not able to measure its value (Lambros, 1999).

By means of the domain integral method values of K_I, K_{II} and T corresponding to the experimentally recorded instant of crack initiation were calculated for each specimen evaluated. A very fine mesh near the crack tip was used in all the specimens since the standard domain integral must be evaluated in a region sufficiently small around the crack tip to maintain the path independence of the *J*-integral in a non-homogeneous material (Gu, 1997). The entire specimens were modeled by means of approximately 30000 CPS8R elements. An example of the mesh used in the simulations is shown in Fig. 2 and computed values of the fracture parameters for each specimen analyzed are shown in Table 2. Experimental results and results obtained numerically by the same authors in collaboration with other researchers in a related work (Oral, 2008) are also shown for comparison purposes.

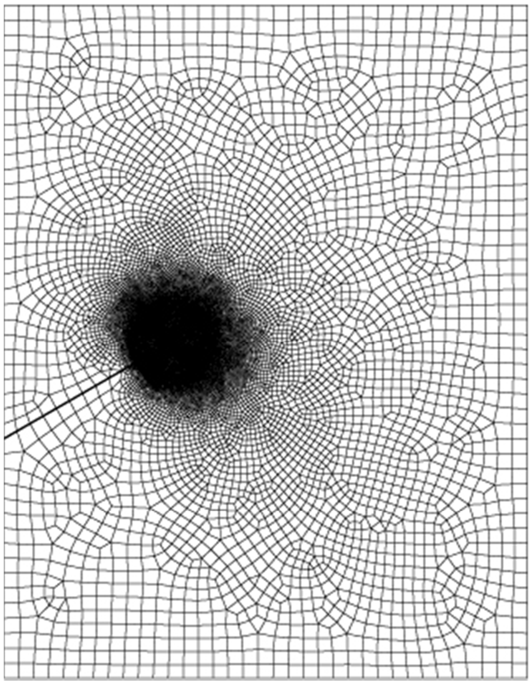

Fig.2 Representative finite element mesh

Table 2 Experimental and numerical results for K_I, K_{II} and the *T*-stress for each FGM specimen

	Results	Case	K_I [MPa m$^{0.5}$]	K_{II} [MPa m$^{0.5}$]	T [MPa]
Expt.	Abanto-Bueno & Lambros (Abanto-Bueno, 2006)	I	0.554	0.039	-4.272
Num.	Oral et. al (Oral, 2008)	I	0.551	-0.022	-2.149
	Present	I	0.589	-0.011	-1.538
Expt.	Abanto-Bueno & Lambros (Abanto-Bueno, 2006)	II	0.755	0.179	-0.069
Num.	Oral et. al (Oral, 2008)	II	0.722	0.204	-0.673
	Present	II	0.734	0.257	-0.539
Expt.	Abanto-Bueno & Lambros (Abanto-Bueno, 2006)	III	0.969	0.224	-0.930
Num.	Oral et. al (Oral, 2008)	III	0.878	0.230	-0.870
	Present	III	0.908	0.304	-0.763

As seen in Table 2, results agree reasonably well with the experimental data, although there are some differences that need to be examined. The greatest discrepancies arise in the *T*-stress that, being a second-order term, is more difficult to extract, both numerically and experimentally. Besides, results are affected by the different procedures chosen to extract them and Abanto-Bueno and Lambros, in both their experimental (Abanto-Bueno, 2006) and their related numerical work (Oral, 2008), fit the experimentally measured or numerically computed displacements in the asymptotic displacement equation to obtain the value of the fracture parameters, while in this work these are computed by means of the Domain Integral.

Also, a negative value of K_{II} is obtained in the first case, in contraposition with the positive value extracted from the experiments. The value is relatively small and whence the difference is minimal, but the sing affects the direction of crack kinking. The crack growth analysis conducted by Abanto-Bueno and Lambros (Abanto-Bueno, 2006) shows a positive kink direction and therefore, the negative sign of K_{II} obtained in the present simulation correctly predicts the positive sign of subsequent crack kinking. So that, given the unavoidable experimental error and taking into account the above considerations, one could conclude that the similarity with the experimental results is more than enough to validate the finite element simulations.

Once validated, the numerical model is developed to analyze the influence of a spatial variation of the Poisson's ratio on the results. In order to do so, fracture parameters are computed for different constant Poisson's ratios and for a continuously variation of its value. Values considered for the Poisson's ratio range from 0.1 to 0.45, the amount assumed in the experimental work. Notice that in FGMs, variations of Poisson's ratio and Young's modulus have opposite orientations.

RESULTS

Case I – FGMI

Table 3 shows fracture parameters computed for various constant Poisson's ratios in the first graded specimen, where tension load is applied in the direction parallel to material gradation and mixed-mode loading is induced by placing the crack line at an angle to the direction of mechanical property variation.

Table 3 Fracture parameters obtained for various constant Poisson's ratios in FGMI

Poisson's ratio	K_I [MPa $m^{0.5}$]	K_{II} [MPa $m^{0.5}$]	T [MPa]
ν=0.1	0.590	-0.016	-1.540
ν=0.2	0.589	-0.015	-1.539
ν=0.3	0.589	-0.013	-1.539
ν=0.4	0.589	-0.012	-1.538
ν=0.45	0.589	-0.011	-1.538

As it could be expected, since the configuration corresponds to the most susceptible to changes in the Poisson's ratio, all fracture parameters are sensitive to its value, being this particularly significant for K_{II} in the geometry and crack location considered. Values obtained for the SIFs and the *T*-stress considering a continuously variation of the Poisson's ratio through the specimen are shown in Table 4.

Table 4 Fracture parameters obtained for a continuously variation of the Poisson's ratio in FGMI

Poisson's ratio	K_I [MPa m$^{0.5}$]	K_{II} [MPa m$^{0.5}$]	T [MPa]
ν=0.1→0.45	0.589	-0.003	-1.537
ν=0.45	0.589	-0.011	-1.538

Results shown in Table 4 are in line with those reported in Table 3 and confirm the inaccuracies arising in the fracture parameters calculation when assuming a constant Poisson's ration in this configuration, being this clearly observed in the term K_{II}.

Case II – FGMII

SIFs and *T*-stresses obtained for various constant Poisson's ratios in FGMII, where tension load is applied in the direction perpendicular to material gradation and mode mixity is a result of both loading and material gradient asymmetry, are shown in Table 5.

Table 5 Fracture parameters obtained for various constant Poisson's ratios in FGMII

Poisson's ratio	K_I [MPa m$^{0.5}$]	K_{II} [MPa m$^{0.5}$]	T [MPa]
ν=0.1	0.734	0.257	-0.532
ν=0.2	0.734	0.257	-0.534
ν=0.3	0.734	0.257	-0.536
ν=0.4	0.734	0.257	-0.538
ν=0.45	0.734	0.257	-0.539

Results show that the Poisson's ratio effect on the SIFs can be neglected for this configuration, in agreement with Delale and Erdogan's conclusions (Delale, 1983), but the nonsingular term of the *T*-stress shows sensitivity to the changes in Poisson's ratio value. Table 6 shows the fracture parameters calculated assuming a continuously variation of the Poisson's ratio.

Table 6 Fracture parameters obtained for a continuously variation of the Poisson's ratio in FGMII

Poisson's ratio	K_I [MPa m$^{0.5}$]	K_{II} [MPa m$^{0.5}$]	T [MPa]
ν=0.1→0.45	0.734	0.257	-0.549
ν=0.45	0.734	0.257	-0.539

Table 6 proves that, when tension load is applied in the direction perpendicular to the material gradient, Poisson's ratio variation must be considered when computing the *T*-stress term, whereas its effect on the SIFs can be neglected.

Case III – FGMIII

In the third specimen, mixed mode fracture is attained by asymmetric external loading and tension load forms an angle with the material gradient. Therefore, this geometry shows an intermediate case between the more and less favourable configurations for the Poisson's ratio effect. Fracture parameters computed for various constant Poisson's ratios and a continuously variation of its value are shown in Tables 7 and 8 respectively.

Table 7 Fracture parameters obtained for various constant Poisson's ratios in FGMIII

Poisson's ratio	K_I [MPa m$^{0.5}$]	K_{II} [MPa m$^{0.5}$]	T [MPa]
ν=0.1	0.911	0.301	-0.771
ν=0.2	0.910	0.302	-0.768
ν=0.3	0.909	0.303	-0.766
ν=0.4	0.908	0.304	-0.764
ν=0.45	0.908	0.304	-0.763

Table 8 Fracture parameters obtained for a continuously variation of the Poisson's ratio in FGMIII

Poisson's ratio	K_I [MPa m$^{0.5}$]	K_{II} [MPa m$^{0.5}$]	T [MPa]
ν=0.1→0.45	0.906	0.306	-0.756
ν=0.45	0.908	0.304	-0.763

Results show the influence of the Poisson's ratio in both the SIFs and the *T*-stress.

CONCLUSION

Considering the overall results for the three specimens, these show a high dependence on geometry of the Poisson's ratio effect. Thereby, its influence on the SIFs can only be neglected when load is applied in the direction perpendicular to material gradation, and if the analysis includes the computation of the *T*-stress term, Poisson's ratio variation must be taken into account independently of the configuration evaluated.

ACKNOWLEDGMENTS

The authors gratefully acknowledge the funding by Ministerio de Ciencia e Innovación of Spain through the project DPI2010.21590.C02.01.

REFERENCES

Abanto-Bueno J, Lambros J. An experimental study of mixed mode crack initiation and growth in functionally graded materials. Experimental Mechanics, 2006, 46, p. 179-196.

Delale F, Erdogan F. The crack problem for a nonhomogeneous plane. Journal of Applied Mechanics, 1983, 50 (3), p. 609-614.

Gu P, Dao M, Asaro RJ. A simplified method for calculating the crack-tip field of functionally graded materials using the domain integral. Journal of Applied Mechanics, 1997, 34 (1), p. 1-17.

Lambros J, Santare MH, Li H and Sapna GH. A novel technique for the fabrication of laboratory scale model functionally graded materials. Experimental Mechanics, 1999, 39 (3), p. 184-190.

Paulino GH, Kim J.-H. On the Poisson's ratio effect on mixed-mode stress intensity factors and T-stress in functionally graded materials. International Journal of Computational Engineering Science, 2004, 5 (4), p. 833-861.

Rousseau CE, Tippur HV. Compositionally graded materials with cracks normal to the elastic gradient. Acta Materialia, 2000, 48, p. 4021-4033.

Tilbrook MT, Moon RJ, Hoffman M. Crack propagation in graded composites. Composites Science and Technology, 2005, 65, p. 201-220.

Oral A, Lambros J, Anlas G. Crack initiation in functionally graded materials under mixed mode loading: experiments and simulations. Journal of Applied Mechanics, 2008, 75 (5), p. 0511101 (8 pages).